Title
Preparation and Characterization of High-Surface-Area Bi(1–x)/3V1–x Mo x O4 Catalysts

Journal
Langmuir, 30(3)

ISSN
0743-7463

Authors
Nell, Alexandre
Getsoian, Andrew Bean
Werner, Sebastian
et al.

Publication Date
2014-01-28

DOI
10.1021/la403646g

Peer reviewed

Langmuir

Article

pubs.acs.org/Langmuir

Preparation and Characterization of High-Surface-Area $Bi_{(1-x)/3}V_{1-x}Mo_xO_4$ Catalysts

Alexandre Nell,[†,‡] Andrew "Bean" Getsoian,[†] Sebastian Werner,[†] Lioubov Kiwi-Minsker,[‡] and Alexis T. Bell*[,†]

[†]Department of Chemical and Biomolecular Engineering, University of California—Berkeley, Berkeley, California 94720-1462, United States

[‡]Ecole Polytechnique Fédérale de Lausanne, Institut des Sciences et Ingénierie Chimiques, CH-1015 Lausanne, Switzerland

Supporting Information

ABSTRACT: We report the successful application of a templating approach employing ordered mesoporous carbon to the synthesis of $BiVO_4$, $Bi_2Mo_3O_{12}$, and $Bi_{0.85}V_{0.55}Mo_{0.45}O_4$ and the performance of these materials as catalysts for the oxidation of propene to acrolein. Ordered mesoporous carbon templates were used to control the nucleation and growth of the mixed metal oxide crystals, allowing higher final surface areas to be obtained. The resulting materials were characterized by X-ray diffraction, Raman spectroscopy, transmission electron microscopy, X-ray photoelectron spectroscopy, and BET surface area analysis. The surface area of the mixed metal oxide catalysts was found to depend on the type of mesoporous silica used to prepare the carbon template and on the conditions under which the carbon template was formed. Through an appropriate choice of template, the surface areas of the mixed metal oxides exceeded 15 m^2/g. Catalytic testing revealed that materials produced via templating in ordered mesoporous carbon had per-gram activities that were up to 85 times higher than those produced by a conventional hydrothermal synthesis and exhibited stable catalytic activities over 24 h.

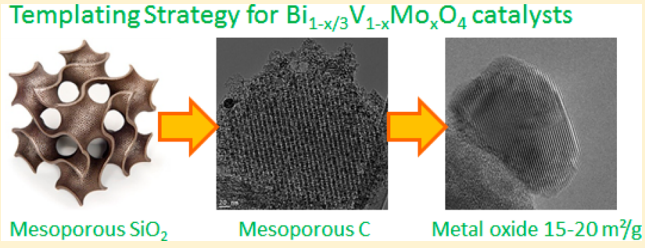

INTRODUCTION

Oxides containing bismuth in combination with vanadium and molybdenum are used as catalysts for the oxidation of hydrocarbons and alcohols and for the photo- and electrochemical oxidation of water. For example, bismuth vanadate shows great promise as a photocatalyst for the splitting of water into hydrogen and oxygen.[1,2] Catalysts based on bismuth molybdate have long been used for the selective oxidation and ammoxidation of olefins to aldehydes and nitriles.[3−5] It has also been observed that the substitution of vanadium for molybdenum in such materials lowers the activation barrier and increases the rate of propene oxidation without changing the selectivity to acrolein.[6,7] In catalysts used industrially for olefin functionalization, however, the phases responsible for catalytic activity are found to have very low surface areas, typically 1 to 2 m^2/g.[8−10] Because catalysis is a surface phenomenon, there is considerable interest in developing methods for preparing such oxides with high surface area.

Most of the strategies investigated for increasing the surface areas of bismuth vanadates and molybdates have focused on changing the conditions in the commonly used hydrothermal approach. Beale and Sankar[11] have found that three phases of bismuth molybdate can be formed at temperatures below 200 °C and that the phase formed is more strongly dependent on the pH at which the synthesis is carried out than on the ratio of the bismuth and molybdenum precursors in solution. A surface area of 8.9 m^2/g was attained for the as-prepared material, decreasing only slightly to 8.2 m^2/g after 4 h of calcination at 400 °C. Le et al.[8,9] have investigated both complexation and spray drying as methods for improving the surface areas of bismuth molybdate. Using a 3:1 ratio of citric acid to bismuth, a pH near 1, and a calcination temperature of 500 °C, they were able to obtain surface areas of ∼12 m^2/g for $Bi_2Mo_3O_{12}$. Spray drying was also found to be effective at increasing the surface area of $Bi_2Mo_3O_{12}$, particularly when used in conjunction with citric acid complexation; however, the best result by this approach did not exceed 8 m^2/g. Changing the complexing agent from citrate to malonate, malate, sorbital, or dimethyl oxalate was also considered. Sorbital gave the best results, followed by citrate, but again, surface areas did not exceed 10 m^2/g. A particularly interesting synthesis approach has been reported by Ghule et al.,[12] who produced nanorods of $Bi_2Mo_3O_{12}$ by taking bismuth molybdate particles prepared by precipitation from aqueous solution and subjecting them to 6 h of sonication in a pyridine solution, followed by calcination at 450 °C. Although the surface area of the final product was not reported, the surface area of a 10 nm × 500 nm bismuth molybdate nanorod is estimated to be ∼65 m^2/g. The authors do note, however, that the nanorod structures degrade with the formation of other phases upon exposure to moisture.

Received: September 25, 2013
Revised: January 8, 2014
Published: January 8, 2014

The effect of pH on the hydrothermal synthesis of $BiVO_4$ has been investigated by Yu and Kudo,[2] who found that surface areas of 0.5−2.6 m^2/g could be obtained for starting solutions ranging in pH from 1 to 9. These authors also observed that the addition of ammonia to the synthesis liquor produced a $BiVO_4$ phase that after calcination had a surface area of 22 m^2/g. However, this material was amorphous, had completely different light absorption properties than crystalline $BiVO_4$, and was inactive for the photocatalytic evolution of oxygen from aqueous $AgNO_3$ solution. Ren et al.[13] have investigated the solvothermal synthesis of $BiVO_4$ using water−ethanol mixtures heated to 160 °C. By varying the water to ethanol ratio, they were able to generate a variety of different particle morphologies, several of which had BET surface areas of 10−11 m^2/g. A promising procedure for increasing surface areas has been proposed by Li et al.,[14] who investigated the use of mesoporous silicas as templates for $BiVO_4$ synthesis. In a typical synthesis, a dry silica template was stirred with an ethanol and nitric acid solution of $Bi(NO_3)_3{\cdot}5H_2O$ and NH_4VO_3, which impregnated the pores of the silica by capillary action over the course of 12 h. The impregnated silica was then calcined at 200 °C for 12 h, and the framework was removed by etching in 2 M NaOH. Several mesoporous silica templates were tested, including KIT-6, SBA-15, and SBA-16. Of these, KIT-6 produced materials with the highest surface areas. The authors attribute this to the presence of large, three-dimensionally connected pores in the KIT-6 structure. $BiVO_4$ produced through KIT-6 templating could be synthesized with surface areas as great as 59 m^2/g, and the resulting catalysts showed excellent photocatalytic activity for both gas-phase NO oxidation and aqueous-phase decomposition of methylene blue.

In addition to mesoporous silicas, ordered mesoporous carbon materials have also been investigated as templates for the synthesis of metal oxides. Ordered mesoporous carbons are themselves templated from mesoporous silicas, as extensively detailed by Ryoo and co-workers.[15−17] Kondo has examined the use of carbon templates to stabilize already-synthesized mesoporous oxides during crystallization.[18] The synthesis of nanosized metal oxide particles inside ordered mesoporous carbon supports has been investigated by several researchers for applications in electrochemistry.[19,20] The templating of metal oxides through the impregnation of ordered mesoporous carbon CMK-3 (produced using mesoporous silica SBA-15), followed by the oxidative removal of the carbon template, has been reported for the production of mesoporous CuO,[21] MgO,[22] and ZnO.[23]

In this article, we report the use of mesoporous silica KIT-6 and ordered mesoporous carbons CMK-1 and CMK-8 as templates for the synthesis of high-surface-area $BiVO_4$, $Bi_{0.85}V_{0.55}Mo_{0.45}O_4$, and $Bi_2Mo_3O_{12}$ catalysts. The effects of the choice of the mesoporous silica template, carbonization atmosphere, and temperature ramp rate during catalyst calcination on the surface areas of $BiVO_4$, $Bi_{0.85}V_{0.55}Mo_{0.45}O_4$, and $Bi_2Mo_3O_{12}$ catalysts were investigated. We also investigated the catalytic activity, selectivity, and stability of these materials for the selective oxidation of propene to acrolein and compare the properties with those for their conventionally prepared low-surface-area counterparts.

EXPERIMENTAL METHODS

Catalyst Preparation. Mesoporous silicas KIT-6[24] and MCM-48[25] were prepared according to procedures described in the literature. MCM-48 had a surface area of ∼1520 m^2/g and a pore volume of 0.87 cm^3/g, and KIT-6 had surface areas of between 780 and 880 m^2/g and pore volumes between 0.91 and 1.93 cm^3/g. The surface area and pore volume of both materials are in good agreement with values reported originally.[18,19] Impregnation of the silica templates with a carbon precursor was done according to the recommendations of Joo et al.[14−16] A solution of 1.25 g of sucrose (Fischer Scientific) was dissolved in 5 mL of 0.25 N sulfuric acid (Fischer Scientific) and used to carry out the incipient wetness impregnation of 1 g of dried silica. The uptake volume varied from 2.9 to 3.6 mL for MCM-48 and between 3.6 and 3.8 mL for KIT-6, slightly lower than the 5.0 mL/g expected from the work of Joo et al. The impregnated silica was dried for 2 h at 80 °C and then overnight at 160 °C. A second impregnation step was carried out using a solution of 0.75 g of sucrose in 5 mL of 0.25 N sulfuric acid for which the uptake volume varied from 2.4 to 2.6 mL for MCM-48 and from 3.8 to 4.2 mL for KIT-6. The twice-impregnated silica was again dried at 80 and 160 °C and then carbonized at 760 °C for 12 h in a horizontal tube furnace under flowing Ar (99%, Praxair) or H_2 (10% in He, Praxair).

The silica template was removed from the mesoporous carbon by treatment with ammonium bifluoride. A stock solution containing 20 mL of NH_3 (28%, Sigma-Aldrich) and 20 mL of HF (48%, EMD) in 415 mL of filtered water (Millipore) was carefully[26] prepared. To extract 1 g of silica from the mesoporous carbon, the carbon-impregnated silica was stirred in 200 mL of ammonium bifluoride for 20 min at room temperature and then filtered and repeatedly rinsed with water. The buffered solution was immediately neutralized with calcium carbonate.

Bismuth vanadate, bismuth molybdate, and bismuth vanadate-molybdate catalysts were prepared by an adaptation of the method of Li et al.[13] Typically, 0.67−1.00 mmol of $Bi(NO_3)_3{\cdot}5H_2O$ (99.99%, Sigma-Aldrich) was dissolved in a mixture of 1 mL of nitric acid (67%, EMD) and 3 mL of ethanol (99.8% from extractive rectification; contains traces of toluene). Once the bismuth precursor was completely dissolved, an additional 7 mL of ethanol was added, followed by the introduction of appropriate molar proportions of NH_4VO_3 (99%, Fluka) and $(NH_4)_6Mo_7O_{24}{\cdot}4H_2O$ (99.98%, Sigma-Aldrich). It was found that strict adherence to the order of addition given here was essential in order to obtain stable, clear solutions.

The precursor solution was contacted with freshly dried mesoporous carbon and allowed to absorb into the pores over the course of 12 h at 60 °C. The resulting material was then calcined at 200 °C for 12 h in air to decompose the ammonium and nitrate precursors and subsequently at 380 °C for 6 h to fully remove the carbon template.

Additional samples were prepared by impregnating the ethanolic precursor solution directly into freshly dried KIT-6. The same drying and calcination procedure was applied, followed by removal of the KIT-6 framework using either 2.0 or 0.1 M KOH or 0.01 M NH_4HF_2.

A third set of samples were synthesized by citric acid complexation of the Bi, Mo, and V precursors. The resulting solutions were dried at 80 °C, decomposed at 150 °C, and then calcined in air (zero grade, Praxair) for 6 h at 600 °C.

Catalyst Characterization. XPS analysis was performed using a PHI 550 spectrometer equipped with an Al Kα anode operating at 1486.7 eV and 350 mW. Samples were prepared by pressing catalyst powder into double-sided conductive copper tape (Ted Pella), the reverse of which was mounted to a stainless steel sample holder. The instrument base pressure was $<1 \times 10^{-8}$ Torr.

BET analysis was performed using a Micromeritics Gemini VII surface area and pore volume analyzer. An attempt was made to load enough sample into the instrument to provide at least 2 m^2 of total surface area for analysis. However, the sample tube volume limited the total catalyst loading to ∼2 g, resulting in somewhat less than 2 m^2 of total surface area being available in the analysis of samples made by citrate complexation.

Thermogravimetry analysis was carried out using an SII Exstar 6000. Aluminum pans were loaded with 2−10 mg of sample and ramped at 2 °C/min to 500 °C in air.

dx.doi.org/10.1021/la403646g | Langmuir 2014, 30, 873−880

X-ray diffraction patterns were obtained with a Siemens D5000 diffractometer using Cu Kα radiation. The data were collected in the range of $10° < 2\theta < 70°$ in increments of 0.02°.

Transmission electron microscopy was performed with a monochromated FEI Tecnai T20 microscope (C_s = 0.5 mm, C_c = 1.1 mm) at 200 kV equipped with a field-emission gun and a Gatan imaging filter (GIF). HR-TEM images were collected using a C_2 aperture of 150 μm. Energy-filtered TEM was performed using the energy filter at the GIF calibrated to C at 284.5 eV. EF-TEM images were acquired using an objective aperture of 60 μm and a C_2 aperture of 300 μm. An energy slit of 5 eV was aligned using the zero-loss peak and subsequently shifted to the desired range. For elemental maps, an appropriate edge was selected and the beam was focused. For O, the K edge at 543.1 eV; for V, the $L_{2,3}$ edge at 519.8 eV; for Mo, the $M_{4,5}$ edge at 506.3 eV; and for Bi, the $O_{2,3}$ edge at 92.6 eV were used. Typical exposure times were 20 s for O, V, and Mo and 10 s for Bi. Elemental maps were computed by digital micrograph using the cross-correlation method between two pre-edge images and one postedge image. Samples were prepared by wet milling 5 mg of the sample powder in 2 mL of hexane (ACS grade, Aldrich) and sonicating for 5 min. Subsequently, 5 μL was drip coated onto a lacey carbon grid (Electron Microscopy Science, Cu-300) and dried in air.

Raman spectra were acquired using a Jobin Yvon confocal Raman spectrometer equipped with a 532.1 nm Nd/YAG laser operating at a nominal power of 17 mW. Typically, a neutral density filter was used to reduce the power to 0.17 mW before analysis.

Catalytic testing was performed in a system described in detail by Zheng et al.[7] Catalysts were loaded into a quartz tube reactor and pretreated for 12 h at 400 °C in oxygen (20% in He, Praxair). Reactions were run at atmospheric pressure using a 1:1 ratio of oxygen to propene (99.9%, Praxair) diluted in He (99.99%, Praxair). The partial pressures of O_2 and propene were each 0.167 atm, and the total flow rate was 60 mL/min. Reaction products were analyzed by gas chromatography using an HP-PLOT-Q column with a flame ionization detector for the analysis of propene, acrolein, acetic acid, acetaldehyde, and ethane and an Allstech Hayesep DB column and thermal conductivity detector for the analysis of oxygen, carbon monoxide, and carbon dioxide.

RESULTS AND DISCUSSION

Characterization and Testing of Catalysts Prepared Using a Silica Template. The Raman spectrum of $Bi_{0.85}V_{0.55}Mo_{0.45}O_4$ prepared using KIT-6 as the template is shown in Figure 1 (bottom, black). The BET surface area of this material was 15 m^2/g. Shown for comparison is the spectrum of a catalyst of identical composition prepared by citrate complexation (Figure 1, middle, blue). The two spectra are essentially identical, confirming that a bulk $Bi_{0.85}V_{0.55}Mo_{0.45}O_4$ phase had been produced. XRD spectra confirmed this conclusion (not shown). The spectra are consistent with those previously reported in the literature.[27]

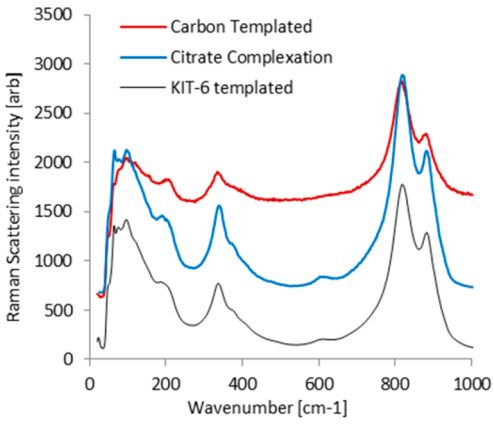

Figure 1. Raman scattering spectra of $Bi_{0.85}V_{0.55}Mo_{0.45}O_4$ templated from KIT-6 followed by removal of the template with 0.1 M NaOH (bottom, black) and templated from mesoporous carbon followed by removal of the template by calcination in air at 400 °C (top, red) compared to that of $Bi_{0.85}V_{0.55}Mo_{0.45}O_4$ produced by citrate complexation (middle, blue).

The materials made in this fashion exhibited no catalytic activity for the oxidation of propene, and neither acrolein nor CO_x was detected at 400 °C. The cause of this surprising result was explained by XPS analysis: signals indicative of the presence of vanadium and molybdenum were completely absent from the XPS spectrum, and only signals indicative of bismuth and oxygen were found. This observation suggests that the removal of the silica template resulted in the formation of a bismuth oxide phase on the surface. Although Bi_2O_3 is known to be active for the aromatization of propene to benzene at higher temperatures,[28] it is not active for the oxidation of propene at 400 °C. Either molybdenum or vanadium must be present on the catalyst surface along with bismuth in order for acrolein to be formed.[7,29,30]

A similarly inactive catalyst was obtained when $Bi_{0.85}V_{0.55}Mo_{0.45}O_4$ prepared by the citrate complexation method was stirred in 2.0 M aqueous KOH for 30 min and then filtered, rinsed with deionized water, and dried. XPS analysis of the KOH-treated sample also indicated the total disappearance of V and Mo from the catalyst surface. A second attempt was made to remove the silica template from a KIT-6-templated $Bi_{0.85}V_{055}Mo_{0.45}O_4$ sample using 0.1 M KOH. The XPS spectrum of this material showed only weak features for V and Mo (Figure 2, blue). More dilute solutions of KOH could not be used because below 0.1 M the pH is too low to dissolve the silica template.[31] Consistent with this observation, Figure 2 shows that even after 30 min of exposure to 0.1 M KOH solution a residual Si peak can be seen. On the basis of these results, it was concluded that the removal of the silica template by dissolution in base could not be used to produce a product with surface composition representative of the bulk $Bi_{0.85}V_{0.55}Mo_{0.45}O_4$ stoichiometry.

The only alternative to base for removing silica is the use of fluoride ions. The rate of dissolution of silica in HF has been studied as a function of pH,[32] and the optimal rate has been found to occur when pH = pK_a(HF) = 3.3. Studies have suggested that the $[FHF^-]$ ion is the active species involved in silica dissolution.[33,34] Thus, an attempt was made to remove the silica template in an ammonium bifluoride solution with a pH of 3.3. Initially an $[F^-]$ concentration of 0.1 M was used. The XPS spectrum of the resulting catalyst showed that V and Mo were present in addition to Bi; however, a large peak for residual F was also present. This result suggests that whereas fluoride ions do not dissolve V or Mo at pH 3.3 they do strongly bind to the catalyst surface. An attempt to reduce the level of fluoride attachment to the catalyst surface was made by reducing the F^- concentration to 0.01 M. As seen in the top spectrum in Figure 2 (red), a small residual F 1s peak remained visible near 680 eV even after repeated rinsing with water. Because fluoride dissolves silica stoichiometrically to produce SiF_6^{2-} ions, further dilution of the fluoride was deemed impractical because of the very large volumes of fluoride solution that would have been required to achieve complete dissolution of the silica. Given the difficulties encountered in template removal by either hydroxide or fluoride, templating metal oxides in mesoporous silica was deemed unsuitable for

dx.doi.org/10.1021/la403646g | Langmuir 2014, 30, 873−880

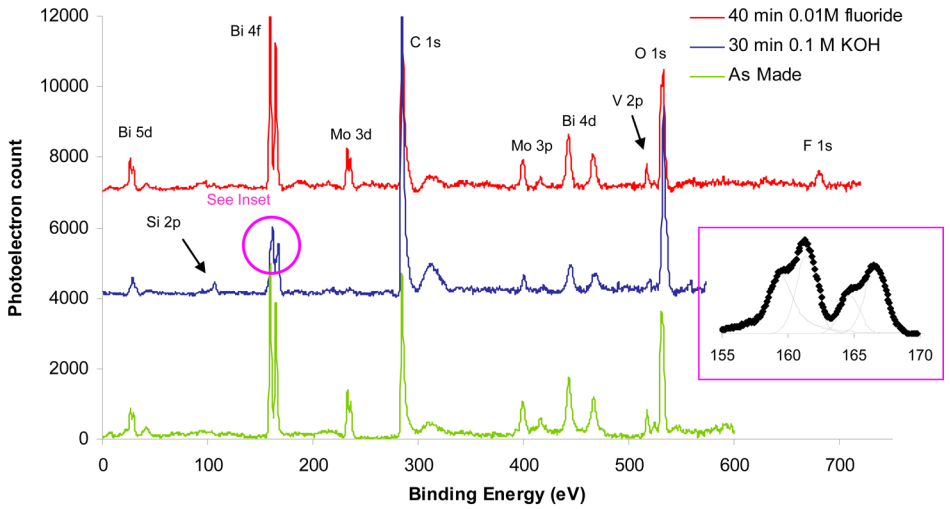

Figure 2. XPS spectra of $Bi_{0.85}V_{0.55}Mo_{0.45}O_4$ catalysts prepared by (bottom) citrate complexation, (middle) templating in KIT-6 followed by treatment with 0.1 M KOH, and (top) templating in KIT-6 followed by treatment with 0.01 M NH_4HF_2. Splitting of the Bi 4f peaks indicating the formation of Bi^{5+} on the surface in the KOH-treated sample is shown in the inset.

the preparation of bismuth vanadate–bismuth molybdate solid solution catalysts and was not pursued further.

Characterization of Catalysts Prepared Using a Carbon Template. The effect of the gas composition under which the carbonization of sucrose-impregnated MCM-48 or KIT-6 was carried out on the surface areas of the mesoporous carbon templates produced is shown in Table 1. The surface area of CMK-1 produced from sucrose-impregnated MCM-48 increased from 930 m^2/g when carbonized in 10% H_2 in He to ~1100 m^2/g when carbonized in Ar, whereas the surface area of CMK-8 produced from sucrose-impregnated KIT-6 increased from ~1530 m^2/g for carbonization under H_2 to ~1750 m^2/g for carbonization under Ar. The surface area of CMK-1 is lower than that of the MCM-48 template used to produce it (~1550 m^2/g), whereas the surface area of CMK-8 is roughly twice that of the KIT-6 template used to produce it. The result for CMK-8 was unexpected because CMK-1 and CMK-8 reported by Ryoo and co-workers[13] had surface areas similar to those of the silica templates used to create them; the largest surface area they report for a CMK material is 1250 m^2/g. The high surface areas obtained here may be attributable to the differences in carbonization conditions between the two studies. Ryoo et al. used carbonization temperatures of 900–2400 °C and performed carbonization under vacuum, whereas a temperature of 760 °C and an argon or hydrogen/helium atmosphere was used for carbonization in the present study. TEM images of Ar-CMK-1 and Ar-CMK-8 were, however, in agreement with those expected from the work of Ryoo et al.[14−16] (Supporting Information).

Table 1. Effect of Template Choice and Carbonization Atmosphere on the Surface Areas of Ordered Mesoporous Carbon Templates[a]

template		carbonization atmosphere	
		H_2/He	Ar
CMK-1 (from MCM-48)	surface area	930	1050–1140
	pore volume	1.46	0.36–0.37
CMK-8 (from KIT-6)	surface area	1520–1540	1760–1790
	pore volume	1.18–1.33	1.05–1.07

[a]Surface areas are in m^2/g using a seven-point BET algorithm. Pore volumes are in cm^3/g using the Dollimore–Heal method. Ranges represent high and low results from multiple trials.

Table 2 lists the surface areas of $BiVO_4$ catalysts prepared using CMK-1 and CMK-8. The highest-surface-area material was produced by templating with CMK-1 carbonized in an Ar atmosphere. The same ordering of metal oxide surface areas H_2/He-CMK-8 < H_2/He-CMK-1 < Ar–CMK-1 was also found for $Bi_{0.85}V_{0.55}Mo_{0.45}O_4$ and $Bi_2Mo_3O_{12}$. However, upon comparison of the results in Tables 1 and 2, there does not appear to be any correlation between the surface area or pore volume of the carbon template and the surface area of the resulting metal oxide. Because the surface area of calcined $BiVO_4$ is roughly 2 orders of magnitude lower than that of the carbon template in which it is produced, it seems likely that the surface area of the oxide is determined to a larger degree by the calcination conditions than by the surface area of the template. Consistent with this conclusion, it was found that the temperatures used to dry the ammonium and nitrate precursor salts and the rate at which the precursor decomposition temperature was attained had a significant effect on the surface area of the $BiVO_4$ produced. Drying the precursor solution at 60 °C and then increasing the temperature to 200 °C at 1 °C/min produced a higher-surface-area oxide than if the precursor was dried at 80 °C and then ramped to 200 °C at 3 °C/min (10.7 m^2/g vs 5.7 m^2/g for H_2/He-CMK-1 templated materials). This result suggests that the mass transport of the evaporating ethanol and gases produced during the decomposition of the ammonium and nitrate salts may cause the pore structure of the oxide or the supporting template to collapse or

Table 2. Effect of Template Choice and Carbonization Atmosphere on the Surface Areas of $BiVO_4$ Catalysts Prepared by Double-Template Synthesis[a]

template	carbonization atmosphere	
	H_2/He	Ar
CMK-1 (from MCM-48)	10.7	15.3
CMK-8 (from KIT-6)	7.0	8.8

[a]Results are in m^2/g.

dx.doi.org/10.1021/la403646g | Langmuir 2014, 30, 873–880

directly pushes the partially formed oxide out of the template mesopores, detrimentally affecting the final surface area.

$BiVO_4$, $Bi_{0.85}V_{0.55}Mo_{0.45}O_4$, and $Bi_2Mo_3O_{12}$ were prepared in Ar-CMK-1, dried at 60 °C, ramped at 1 °C/min to 200 °C, held at 200 °C for 12 h to allow complete decomposition of the ammonium and nitrate precursors, and then calcined at 400 °C for 6 h in air. $BiVO_4$, $Bi_{0.85}V_{0.55}Mo_{0.45}O_4$, and $Bi_2Mo_3O_{12}$ catalysts produced via this method had surface areas of 15, 17, and 14 m^2/g, respectively.

The Raman spectrum of $BiVO_4$ prepared by the carbon-template method is compared to the corresponding pattern for $BiVO_4$ produced by citrate complexation in Figure 3. Also

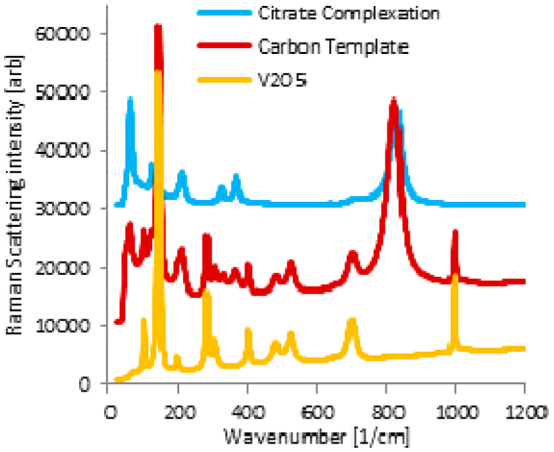

Figure 3. Raman spectra of $BiVO_4$ prepared using a carbon template (red) and by citrate complexation (blue) compared to the Raman spectrum of V_2O_5 (orange).

shown is the Raman spectrum of V_2O_5. It is apparent that some V_2O_5 is present alongside $BiVO_4$ in the sample produced by the carbon-template method. The XRD pattern for $BiVO_4$ produced by carbon templating was very similar to that of $BiVO_4$ produced by citrate complexation, and there was no evidence of V_2O_5 formation in XRD (Supporting Information). This result suggests that Raman spectroscopy is more sensitive than XRD to the presence of small quantities of an impurity phase in this class of materials.

TEM images of $BiVO_4$ produced by carbon-templated synthesis are shown in Figure 4. There is no evidence of porosity in the particles; rather, the higher surface areas obtained from the double-template synthesis procedure appear to arise from the size of the particles produced.

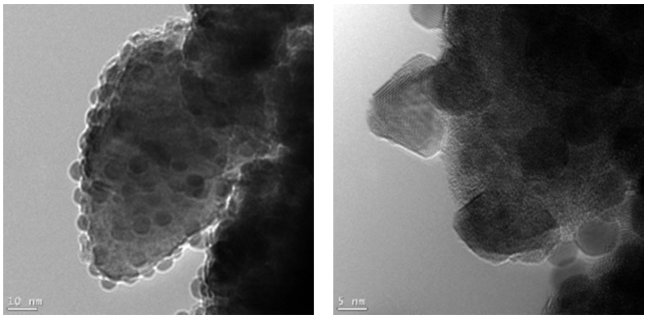

Figure 4. TEM images of $BiVO_4$ produced by carbon-templated synthesis.

The Raman spectrum of $Bi_{0.85}V_{0.55}Mo_{0.45}O_4$ prepared by the carbon-templating method is presented in Figure 1, along with the corresponding spectrum of the material prepared by citrate complexation. The good agreement between the two spectra suggests that no additional phases have been formed during the double-template synthesis of the mixed vanadate−molybdate material. This finding is corroborated by XRD (Supporting Information).

TEM images of $Bi_{0.85}V_{0.55}Mo_{0.45}O_4$ produced by the carbon-template method are shown in Figure 5. The particles are

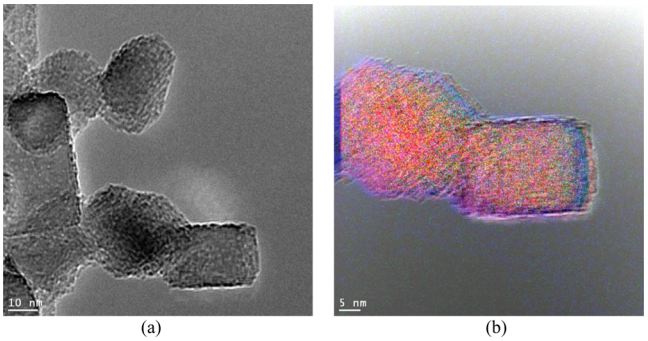

Figure 5. (a) TEM image of a $Bi_{0.85}V_{0.55}Mo_{0.45}O_4$ catalyst prepared by carbon templating. (b) Elemental map of a $Bi_{0.85}V_{0.55}Mo_{0.45}O_4$ particle: bismuth in red, vanadium in green, molybdenum in blue, and oxygen in purple.

approximately rectangular prismatic in shape, with significant surface roughness on the 1 nm scale. Elemental mapping reveals that elements Bi, V, Mo, and O are all dispersed uniformly throughout the bulk of the crystal. An enrichment of the molybdenum signal (blue) at the right edge of Figure 5b is an artifact caused by a slight misalignment of the electron beam during energy sampling at the molybdenum edge.

The Raman spectra of $Bi_2Mo_3O_{12}$ produced by using a carbon template and by citrate complexation are shown in Figure 6. Again, the good agreement between the two spectra

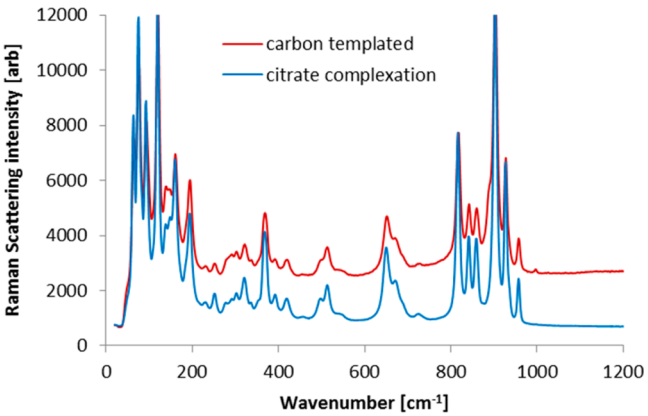

Figure 6. Raman spectra of $Bi_2Mo_3O_{12}$ produced by carbon templating (red) and by citrate complexation (blue).

suggests that no additional phases have formed during the double-template synthesis of $Bi_2Mo_3O_{12}$. This finding was corroborated by XRD (Supporting Information).

TEM images of $Bi_2Mo_3O_{12}$ produced by the carbon-template method are presented in Figure 7. As for $BiVO_4$, no porosity

dx.doi.org/10.1021/la403646g | Langmuir 2014, 30, 873−880

was found, and the higher surface area is a result of the small size of the particles.

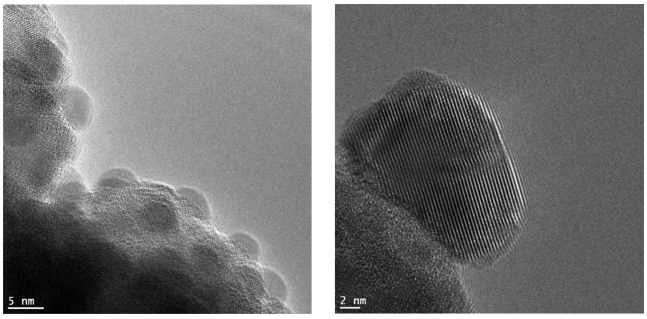

Figure 7. TEM images of $Bi_2Mo_3O_{12}$ produced by carbon-templated synthesis.

The lack of porosity in the mixed metal oxides produced via templating suggests that the quantity of metal oxide precursor used is insufficient to fill the pore volume of the mesoporous carbon; therefore, a fully ordered mesoporous metal oxide is not obtained. Instead, the role of the carbon template can be understood from Figure 8. In the absence of a template, the formation of the mixed metal oxide phase begins when small nuclei (Figure 8a) rapidly grow (b), followed by aggregation (c). Calcination results in large particles (d) with a low surface area per mass. By contrast, in the presence of the template, nucleation takes place within the template pores (e). These pores restrict the growth of the nuclei, allowing a greater number of smaller nuclei to form (f). During calcination, combustion of the template and aggregation and fusion of the nuclei proceed at similar rates (g); the template continues to limit aggregation until it is completely removed. The final metal oxide particles (h) are smaller than those produced in the absence of a template, leading to a greater surface area per mass.

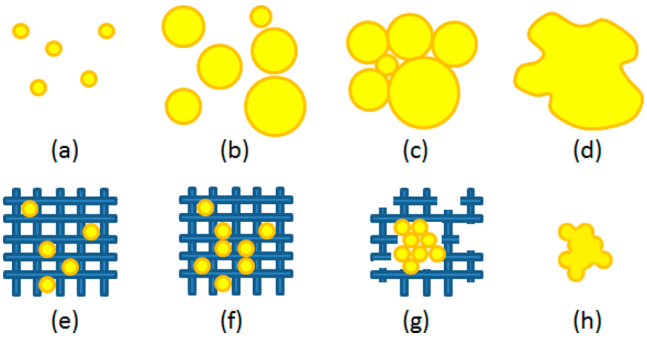

Figure 8. Nucleation and growth of a metal oxide in the absence (a–d) and presence (e–h) of a carbon template. In the absence of a template, initial nuclei (a) rapidly grow (b), coalesce (c), and are converted by calcination to large particles (d) with a low surface area per mass. In the presence of a template, nucleation takes place in the pores of the template (e), which restrict the growth of these nuclei (f), allowing more smaller nuclei to from. During calcination, the nuclei aggregate (g) as the template combusts; the template continues to retard aggregation until it is completely removed. The final metal oxide particles (h) are smaller than those formed without a template, yielding higher surface areas per mass.

Catalytic Performance of Catalysts Prepared Using a Carbon Template. The activity and selectivity of propene oxidation to acrolein exhibited by high-surface-area catalysts prepared using a carbon template were compared to the activity and selectivity of the corresponding low-surface-area catalysts prepared by citrate complexation. As shown in Figure 9, the overall activity of the high-surface-area $BiVO_4$ sample is 80 times greater than that of the low surface area on a mass basis. However, the selectivity to acrolein is only 32% (at roughly 1% conversion) versus 61% selectivity to CO_x. The poor activity and selectivity of this sample can be attributed to the coformation of V_2O_5 during $BiVO_4$ synthesis (Figure 3). V_2O_5 is known to be an active but unselective catalyst for propene oxidation. The activity on a per-mass basis for $Bi_{0.85}V_{0.55}Mo_{0.45}O_4$ is 14 times greater than that of the low-surface-area material, but the distribution of products is nearly identical. The catalytic activity of $Bi_2Mo_3O_{12}$ prepared by the carbon-templating procedure is 85 times higher on a per-mass basis than that of the low-surface-area catalyst. Interestingly, although identical 74% selectivity to acrolein was observed over both the low- and high-surface-area $Bi_2Mo_3O_{12}$ catalysts, a difference was observed in the distribution of byproducts with changes with surface area: the low-surface-area material produces 14% CO and 8% CO_2, but the high-surface-area material produces only 7% CO but 15% CO_2. (A constant 4% selectivity to acetaldehyde was also recorded for each catalyst.) This effect was not observed in $Bi_{0.85}V_{0.55}O_{0.45}O_4$. Because reactions were run under differential (<1%) conversion, an increase in the production of CO_2 does not reflect the partial oxidation of CO on the higher-surface-area catalyst; indeed, $Bi_2Mo_3O_{12}$ does not oxidize CO to CO_2 under these reaction conditions. Because the mechanism by which nonselective products are formed over these catalysts is not known, it is difficult to speculate about the role of surface area in altering the rates of production of CO and CO_2.

Low-surface-area bismuth vanadate–molybdate catalysts are known to be stable under reaction conditions and do not undergo sintering or deactivation. Given the higher surface areas of catalysts made using carbon templates, it was of interest to determine whether their higher surface areas made them more prone to sintering or deactivation. Figure 10 shows the activity and selectivity of the $Bi_{0.85}V_{0.55}Mo_{0.45}O_4$ and $Bi_2Mo_3O_{12}$ catalysts as a function of time on stream. It is observed that the activity and selectivity of both catalysts for the oxidation of propene to acrolein are stable over 24 h, indicating that the higher surface area of these catalysts does not make them more prone to sintering or deactivation under the reaction conditions.

It should also be noted that whereas the per-mass activities of the templated catalysts were significantly greater than those of the corresponding untemplated materials, the activities of the per-surface area were lower: nearly 6-fold lower for $Bi_{0.85}V_{0.55}Mo_{0.45}O_4$ and roughly 3-fold lower for $Bi_2Mo_3O_{12}$. This apparent discrepancy is a result of the pretreatment procedure used prior to catalytic testing: catalysts were held overnight under oxygen at 400 °C prior to carrying out steady-state propene oxidation. Surface areas of the as-prepared catalysts were measured prior to reaction, so any loss of surface area during pretreatment would lead to an apparent lower per-surface-area activity. The mass of catalyst used for steady-state testing (0.01 g) was insufficient for an accurate postreaction surface area measurement. Therefore, larger quantities of $Bi_{0.85}V_{0.55}Mo_{0.45}O_4$ and $Bi_2Mo_3O_{12}$ were separately exposed to oxygen at 400 °C for 12 h in oxygen, after which further surface area analysis was conducted. A 25% decrease in surface area was

dx.doi.org/10.1021/la403646g | Langmuir 2014, 30, 873–880

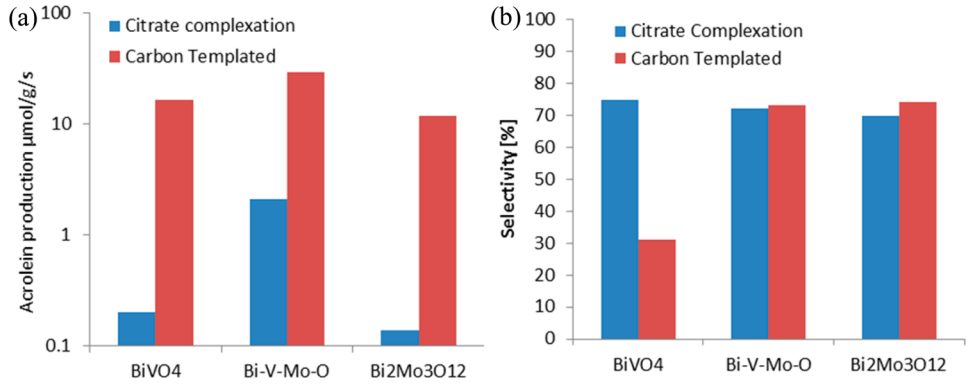

Figure 9. (a) Rate of acrolein production in micromoles of acrolein per gram of catalyst per second for catalysts prepared using carbon templating compared to those prepared by conventional citrate complexation. Note the logarithmic scale. (b) Selectivity to acrolein at ~1% conversion. Reactions are conducted at 400 °C in 0.167 atm O_2, 0.167 atm propene, and 0.667 atm helium.

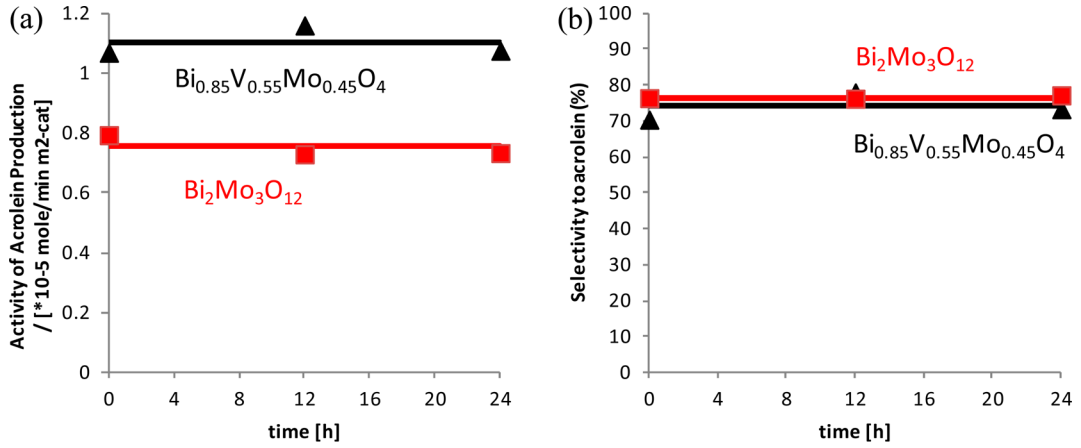

Figure 10. Activity (a) and selectivity (b) of $Bi_{0.85}V_{0.55}Mo_{0.45}O_4$ and $Bi_2Mo_3O_{12}$ catalysts prepared by carbon-templated synthesis after 12 and 24 h on stream. The reaction conditions were maintained at 400 °C, 0.167 atm O_2, 0.167 atm propene, and 0.667 atm He, and the conversion was near 1%.

observed for the $Bi_{0.85}V_{0.55}Mo_{0.45}O_4$ catalyst, and a 10% decrease was observed for $Bi_2Mo_3O_{12}$ as a result of the calcination procedure. Evidently, the catalysts do sinter over 12 h in oxygen alone but not over 24 h when oxygen and propene are both present.

CONCLUSIONS

A procedure utilizing a mesoporous carbon template has been developed for producing bismuth vanadate and bismuth molybdate catalysts with surface areas that are roughly a factor of 2 higher than those reported using nontemplated approaches[2,7−11] and roughly 2 orders of magnitude larger than those obtained by standard citrate complexation synthesis. The highest-surface-area oxides were obtained using mesoporous MCM-48 as the template for the formation of mesoporous carbon CMK-1, followed by removal of the silica template and impregnation of the catalyst precursors in CMK-1. CMK-1 materials carbonized in an argon atmosphere produced higher surface-area oxides than those carbonized in a mixture of hydrogen and helium. Final oxide surface areas of 14−17 m^2/g were obtained for all materials investigated. All of the catalysts showed activity for propene oxidation to acrolein that was 1 to 2 orders of magnitude higher on a per-mass basis than low-surface-area materials with identical composition prepared by citrate complexation. The selectivity to acrolein was the same for high- and low-surface-area $Bi_{0.85}V_{0.55}Mo_{0.45}O_4$ and $Bi_2Mo_3O_{12}$, consistent with the observation that in both cases the catalyst was composed of a single phase. However, in the case of $BiVO_4$, the selectivity to acrolein for the high-surface-area catalyst was significantly lower than that of the low-surface-area catalyst. This difference is attributed to the coexistence of V_2O_5 in the high-surface-area catalyst, which is known to be active for propene oxidation but to exhibit poor selectivity to acrolein. For the three catalyst compositions examined, the high-surface-area materials exhibited no evidence of sintering or deactivation during 24 h under the reaction conditions, but a loss of surface area was observed during 12 h at 400 °C in oxygen.

ASSOCIATED CONTENT

Supporting Information

TEM micrographs of CMK-1 and CMK-8 ordered mesoporous carbon materials and XRD spectra of $BiVO_4$, $Bi_{0.85}V_{0.55}Mo_{0.45}O_4$, and $Bi_2Mo_3O_{12}$ materials made by carbon templating and by citrate complexation. This material is available free of charge via the Internet at http://pubs.acs.org.

AUTHOR INFORMATION

Corresponding Author

*E-mail: bell@uclink.berkeley.edu.

Notes

The authors declare no competing financial interest.

dx.doi.org/10.1021/la403646g | *Langmuir* 2014, 30, 873−880

■ ACKNOWLEDGMENTS

TEM imaging was conducted at the National Center for Electron Microscopy, and XPS data were collected at the Molecular Foundry, both located at Lawrence Berkeley National Laboratory. Support for this work was provided by the U.S. Department of Energy, Office of Basic Science, Chemical Sciences Division, under contract no. DE-AC03-76SF00098.

■ REFERENCES

(1) Sayama, K.; Nomura, A.; Arai, T.; Sugita, T.; Abe, R.; Yanagida, M.; Oi, T.; Iwasaki, Y.; Abe, Y.; Sugihara, H. Photoelectrochemical decomposition of water into H_2 and O_2 on porous $BiVO_4$ thin-film electrodes under visible light and significant effect of Ag ion treatment. *J. Phys. Chem. B* **2006**, *110*, 11352−11360.

(2) Yu, J.; Kudo, A. Effects of structural variation on the photocatalytic performance of hydrothermally synthesized $BiVO_4$. *Adv. Funct. Mater.* **2006**, *16*, 2163−2169.

(3) Grasselli, R. K. Advances and future trends in selective oxidation and ammoxidation catalysis. *Catal. Today* **1999**, *49*, 141−153.

(4) Batist, P. A.; Bouwens, J. F. H.; Schuit, G. C. A. Bismuth molybdate catalysts. Preparation, characterization and activity of different compounds in the Bi-Mo-O system. *J. Catal.* **1972**, *25*, 1−11.

(5) Snyder, T.; Hill, C., Jr. The mechanism for the partial oxidation of propylene over bismuth molybdate catalysts. *Catal. Rev. Sci. Technol.* **1989**, *32*, 43−95.

(6) Ueda, W.; Asakawa, K.; Chen, C. L.; Moro-Oka, Y.; Ikawa, T. Catalytic properties of tricomponent metal oxides having the scheelite structure. *J. Catal.* **1986**, *101*, 360−368.

(7) Zhai, Z.; Getsoian, A.; Bell, A. T. The kinetics of selective oxidation of propene on bismuth vanadium molybdenum oxide catalysts. *J. Catal.* **2013**, *308*, 25−36.

(8) Le, M. T.; van Craenenbroeck, J.; van Driessche, I.; Hoste, S. Bismuth molybdate catalysts synthesized using spray drying for the selective oxidation of propylene. *Appl. Catal., A* **2003**, *249*, 355−364.

(9) Le, M. T.; van Well, W. J. M.; van Driessche, I.; Hoste, S. Influence of organic species on surface area of bismuth molybdate catalysts in complexation and spray drying methods. *Appl. Catal., A* **2004**, *267*, 227−234.

(10) Matsuura, I.; Schut, R.; Hirakawa, K. The surface structure of the active bismuth molybdate catalyst. *J. Catal.* **1980**, *63*, 152−166.

(11) Beale, A. M.; Sankar, G. In situ study of the formation of crystalline bismuth molybdate materials under hydrothermal conditions. *Chem. Mater.* **2003**, *15*, 146−153.

(12) Ghule, A. V.; Ghule, K. A.; Tzing, S.-H.; Chang, J.-Y.; Chang, H.; Ling, Y.-C. Pyridine intercalative sonochemical synthesis and characterization of α-$Bi_2Mo_3O_{12}$ phase nanorods. *Chem. Phys. Lett.* **2004**, *383*, 208−213.

(13) Ren, L.; Ma, L.; Jin, L.; Wang, J.-B.; Qiu, M.; Yu, Y. Tempate-free synthesis of $BiVO_4$ nanostructures: II. Relationship between various microstructures for monoclinic $BiVO_4$ and their photocatalytic activity for the degradation of rhodamine B under visible light. *Nanotechology* **2009**, *20*, 405602.

(14) Li, G.; Zhang, D.; Yu, J. C. Ordered mesoporous $BiVO_4$ through nanocasting: a superior visible light-drivien photocatalyst. *Chem. Mater.* **2008**, *20*, 3983−3992.

(15) Ryoo, R.; Joo, S. H.; Kruk, M.; Jaroniec, M. Ordered mesoporous carbons. *Adv. Mater.* **2001**, *13*, 677−681.

(16) Joo, S. H.; Sun, S.; Ryoo, R. Synthesis of ordered mesoporous carbon molecular sieves CMK-1. *Microporous Mesoporous Mater.* **2001**, *44*, 153−158.

(17) Gierszal, K. P.; Jaroniec, M.; Kim, T.-W.; Kim, J.; Ryoo, R. High temperature treatment of ordered mesoporous carbons produced using various carbon precursors and ordered mesoporous silica templates. *New J. Chem.* **2008**, *32*, 981−993.

(18) Kondo, J. N.; Domen, K. Crystallization of mesoporous metal oxides. *Chem. Mater.* **2008**, *20*, 835−847.

(19) Zhu, S.; Zhou, H.; Hibino, M.; Homma, I.; Ichihara, M. Synthesis of MnO_2 nanoparticles confined in ordered mesoporous carbon using a sonochemical method. *Adv. Funct. Mater.* **2005**, *15*, 381−386.

(20) Li, H.; Wang, R.; Cao, R. Physical and electrochemical characterization of hydrous ruthenium oxide/ordered mesoporous carbon composites as supercapacitor. *Microporous Mesoporous Mater.* **2008**, *111*, 32−38.

(21) Lai, X.; Li, X.; Geng, W.; Tu, J.; Li, J.; Qiu, S. Ordered mesoporous copper oxide with crystalline walls. *Angew. Chem., Int. Ed.* **2007**, *46*, 738−741.

(22) Roggenbuck, J.; Tiemann, M. Ordered mesoporous magnesium oxide with high thermal stability synthesized by exotemplating using CMK-3 carbon. *J. Am. Chem. Soc.* **2005**, *127*, 1096−1097.

(23) Wagner, T.; Waitz, T.; Roggenbuck, J.; Fröba, M.; Kohl, C.-D.; Tiemann, M. Ordered mesoporous ZnO for gas sensing. *Thin Solid Films* **2007**, *515*, 8360−8363.

(24) Kim, T.-W.; Kleitz, F.; Paul, B.; Ryoo, R. MCM-48-like large mesoporous silicas with tailored pore structures: facile synthesis domain in a ternary triblock copolymer-butanol-water system. *J. Am. Chem. Soc.* **2005**, *127*, 7601−7610.

(25) Schumacher, K.; Grün, M.; Unver, K. Novel synthesis of spherical MCM-48. *Microporous Mesoporous Mater.* **1999**, *27*, 201−206.

(26) Concentrated hydrofluoric acid is extremely hazardous. A standard operating procedure for safe handling of this material must be developed and followed, and appropriate personal protective equipment must be worn at all times. A fresh supply of calcium gluconate should be within arms' reach for immediate topical application in case of contact with the skin. See also Kirkpatrick, J. J. R.; Burd, D. A. R. Hydrofluoric acid burns: a review. *Burns* **1995**, *21*, 483−499.

(27) Hartmanova, M.; Le, M. T.; Jergel, M.; Šmatko, V.; Kundracik, F. Structure and electrical conductivity of multicomponent metal oxides having the scheelite structure. *Russ. J. Electrochem.* **2009**, *45*, 621−629.

(28) Swift, H. E.; Bozik, J. E.; Ondrey, J. A. Dehydrodimerization of propylene using bismuth oxide as the oxidant. *J. Catal.* **1971**, *21*, 212−224.

(29) Batist, P. A.; Lippens, B. C.; Schuit, G. C. A. The catalytic oxidation of 1-butene over bismuth molybdate catalysts: II. Dependence of activity and selectivity on the catalyst composition. *J. Catal.* **1966**, *5*, 55−64.

(30) Moro-Oka, Y.; Ueda, W. Multicomponent bismuth molybdate catalysts: a highly functionalized catalyst system for the selective oxidation of olefin. *Adv. Catal.* **1995**, *40*, 233−273.

(31) Wijnen, P. W. J. G.; Beelen, T. P. M.; de Haan, J. W.; Rummens, C. P. J.; van de Ven, L. J. M.; van Santen, R. A. Silica gel dissolution in aqueous alkali metal hydroxides studied by ^{29}Si-NMR. *J. Non-Cryst. Solids* **1989**, *109*, 85−94.

(32) Mitra, A.; Rimstidt, J. D. Solubility and dissolution rate of silica in acid fluoride solutions. *Geochim. Cosmochim. Acta* **2009**, *73*, 7045−7059.

(33) Knotter, D. M. Etching mechanism of vitreous silicon dioxide in HF-based solutions. *J. Am. Chem. Soc.* **2000**, *122*, 4345−4351.

(34) Monk, D. J.; Soane, D. S.; Howe, R. T. A review of the chemical reaction mechanism and kinetics for hydrofluoric acid etching of silicon dioxide for surface micromachining applications. *Thin Solid Films* **1993**, *232*, 1−12.